

Article

Effects of Combined CO₂ and O₃ Exposures on Net CO₂ Assimilation and Biomass Allocation in Seedlings of the Late-Successional *Fagus Crenata*

Hiroyuki Tobita ^{1,*}, Masabumi Komatsu ¹, Hisanori Harayama ², Kenichi Yazaki ¹, Satoshi Kitaoka ¹ and Mitsutoshi Kitao ²

¹ Department of Plant Ecology, Forestry and Forest Products Research Institute, Matsunosato 1, Tsukuba 305-8687, Japan; kopine@ffpri.affrc.go.jp (M.K.); kyazaki@ffpri.affrc.go.jp (K.Y.); skitaoka3104@gmail.com (S.K.)

² Hokkaido Research Center, Forestry and Forest Products Research Institute, Hitsujigaoka 7, Sapporo 062-8516, Japan; harahisa@ffpri.affrc.go.jp (H.H.); kitao@ffpri.affrc.go.jp (M.K.)

* Correspondence: tobi@ffpri.affrc.go.jp

Received: 15 July 2019; Accepted: 21 September 2019; Published: 26 September 2019



Abstract: We examined the effects of elevated CO₂ and elevated O₃ concentrations on net CO₂ assimilation and growth of *Fagus crenata* in a screen-aided free-air concentration-enrichment (FACE) system. Seedlings were exposed to ambient air (control), elevated CO₂ (550 μmol mol⁻¹ CO₂, +CO₂), elevated O₃ (double the control, +O₃), and the combination of elevated CO₂ and O₃ (+CO₂+O₃) for two growing seasons. The responses in light-saturated net CO₂ assimilation rates per leaf area ($A_{\text{growth-CO}_2}$) at each ambient CO₂ concentration to the elevated CO₂ and/or O₃ treatments varied widely with leaf age. In older leaves, $A_{\text{growth-CO}_2}$ was lower in the presence of +O₃ than in untreated controls, but +CO₂+O₃ treatment had no effect on $A_{\text{growth-CO}_2}$ compared with the +CO₂ treatment. Total plant biomass increased under conditions of elevated CO₂ and was largest in the +CO₂+O₃ treatment. Biomass allocation to roots decreased with elevated CO₂ and with elevated O₃. Elongation of second-flush shoots also increased in the presence of elevated CO₂ and was largest in the +CO₂+O₃ treatment. Collectively, these results suggest that conditions of elevated CO₂ and O₃ contribute to enhanced plant growth; reflecting changes in biomass allocation and mitigation of the negative impacts of O₃ on net CO₂ assimilation.

Keywords: allometric relationship; determinant species; leaf aging; stomatal conductance

1. Introduction

Atmospheric carbon dioxide (CO₂) concentrations are predicted to double during the next century, and tropospheric ozone (O₃) levels have also continued to rise globally since pre-industrial times [1–5]. Both CO₂ and O₃ are recognized as anthropogenic air pollutants with opposing impacts on plant growth [6–9]. Elevated CO₂ stimulates plant growth by enhancing photosynthetic carbon assimilation [10–12], although long-term exposure to elevated CO₂ results in photosynthetic down-regulation, especially under limiting nutrient conditions [13,14]. Elevated O₃ concentrations reduce net CO₂ assimilation (A) and accelerate leaf senescence [15,16], potentially resulting in substantial losses of the C-sink strengths in trees [9,17–20].

Elevated CO₂ may alleviate the negative effects of O₃ on photosynthetic activity and plant growth [8,21]. Free-air concentration enrichment (FACE) experiments for CO₂ and other ambient air experiments indicate a nonlinear interaction between plant responses to CO₂ and O₃ [7,22,23]. Hence, O₃ exposure may alter the C metabolism and decrease C stocks for tree species, likely through changes in quantities or the compositions of nonstructural carbohydrates [24]. They may in turn alter C allocation

in plants [19,25]. Increased O₃ concentrations have been shown to shift carbon allocation in favor of aboveground plant tissues, especially leaves, at the expense of root growth, presumably to allocate resources for detoxification and repair of damaged leaves [6,16,26–30]. As elevated CO₂ can alleviate the O₃-induced reduction in *A*, shifts in biomass allocation into leaves may have an over-compensating effect on plant growth under the combination of elevated CO₂ and O₃. Although mechanisms of O₃-induced responses in plants have been revealed [31], responses to elevated O₃ vary widely among species [3,32]. Moreover, interactions between environmental variables such as elevated CO₂, drought, and high temperature, and their effects on crop productivity, are poorly understood [31].

Scaling up from the laboratory to the field with FACE technologies will be crucial to the understanding of plant responses to elevated O₃ and CO₂ [31]. Yet free-air exposure experiments with combinations of elevated CO₂ and O₃ [33] and with elevated O₃ only [17,34,35] are fewer than those performed in free air CO₂ experiments [36–39], especially in Asia [40]. In Japan, free-air CO₂ and O₃ exposure experiments have been conducted under field conditions [41–44]. Kitao et al., [45] reported the growth responses to elevated CO₂ and O₃ in two *Quercus* species, *Q. mongolica* and *Q. serrata*, which have relatively high tolerance to O₃ among Japanese tree species [46,47]. A significant enhancement of growth was observed in the seedlings grown under the combination of elevated CO₂ and O₃, compared with those grown under elevated CO₂ alone. This growth enhancement was considered as an over-compensating response, consisting of two processes: (1) preferential biomass allocation into leaves induced by elevated O₃, and (2) enhanced *A* by elevated CO₂.

Fagus crenata is a representative deciduous broadleaf tree species, widely distributing in the cool temperate forests in Japan [48]. This species is more susceptible to O₃ than the *Quercus* species described above [45]. Even at the current ambient O₃ levels, higher O₃ uptake by a forest of *F. crenata* resulted in an accelerated autumn senescence based on the observations by a flux tower [49]. Previous studies of plant-level *F. crenata* responses to interactions of CO₂ and O₃ produced contradictory results, with one study showing increased growth by combined elevated CO₂ and O₃ in greenhouse experiments [50], and another showing that elevated CO₂ concentrations did not mitigate the negative effects of elevated O₃ on plant growth [51]. Whether elevated CO₂ concentrations ameliorate the negative impacts of O₃ on growth is not certain, even in the same species [52]. To understand growth responses of *F. crenata* to elevated CO₂ and O₃, changes in C allocation into leaves and effects on *A* should be investigated collectively.

Quercus mongolica and *Q. serrata*, mid-successional species with a flush and succeeding-type of leaf emergence [53], can flush new shoots several times under ideal conditions. Unlike these *Quercus* species, *F. crenata*, a shade-tolerant late-successional species [48], has a flush type shoot developmental pattern [53], in which shoots are usually flushed only once in spring. We hypothesized that growth enhancement might be observed in the seedlings of *F. crenata* grown under the combination of elevated O₃ and CO₂, whereas the related growth enhancement is unlikely to be as large as those in the two *Quercus* species [45], because the leaf expansion pattern of *F. crenata* has lower plasticity to changes in environmental conditions. To test this hypothesis, we performed screen-aided FACE experiments and investigated the combined effects of elevated CO₂ and O₃ concentrations on *A* (as a leaf level trait) and biomass allocation (as a plant-level trait) in *F. crenata* seedlings without limiting root growth.

2. Material and Methods

2.1. Experimental Design

Screen-aided free-air concentration enrichment (FACE) experiments with elevated O₃ and CO₂ were performed in the facility used in previous studies [41,45]. The experimental field is located in the nursery of the Forestry and Forest Products Research Institute in Tsukuba, Japan (36°00' N, 140°08' E, 20 m a.s.l.). Plants were exposed to unchanged ambient air (control), elevated CO₂ (+CO₂; 550 μmol mol⁻¹ CO₂), elevated O₃ (+O₃; twice-ambient), or elevated CO₂ and elevated O₃ (+CO₂+O₃; 550 μmol mol⁻¹ CO₂ and twice-ambient O₃). A total of twelve frames (2 m width × 2.5 m height) were

installed with three replicates for each treatment. CO₂ and O₃ were supplied during the daytime with a proportional integral derivative (PID) control system comprised of digital controllers (Model SDC35, Azbil Corporation, Tokyo, Japan). Gaseous CO₂ was obtained from liquid CO₂ (AIR WATER INC., Osaka, Japan). O₃ was supplied by an ozone generator (Model PZ2A; Kofloc, Kyoto, Japan). CO₂ concentration was measured by two CO₂ monitors (Carbon Dioxide Probe, Model GMP343; Vaisala, Helsinki, Finland); in addition, CO₂ concentration in the frames was monitored by an infrared CO₂ analyzer (Model LI-820; LI-COR Inc., Lincoln, NE, USA). Ozone concentration was measured by both an O₃ analyzer (Model EG-3000F; Ebara Jitsugyo Co. Ltd., Kanagawa, Japan) and an O₃ monitor (Model 205; 2B Technologies, Boulder, CO, USA). The exposure periods for CO₂ and O₃ extended from 20 May to 30 November in 2011, and from 25 April to 20 November in 2012 (these data are the same as those reported by Hiraoka et al. [41]). Mean (\pm SE) daytime (7:00–17:00) CO₂ and O₃ concentrations during treatments were 36.1 ± 1.0 and 65.3 ± 2.0 ppb in 2011 and 36.4 ± 0.5 and 61.5 ± 6.2 ppb in 2012 for ambient and elevated O₃, respectively, and were 378 ± 2.5 and 562 ± 16.9 ppm in 2011 and 377 ± 2.9 and 546 ± 21.3 ppm in 2012 for ambient and elevated CO₂, respectively. Frames were surrounded by two transparent windscreens (50 cm height), encircled at 15 and 75 cm above the soil. The windscreens facilitated turbulent mixing of CO₂ and O₃, which were injected with ambient air through holes in vertical polyethylene tubes (2 m in height at 20-cm intervals around the frames) [54]. During the growth seasons from the beginning of April to the end of October in 2011 and 2012, mean monthly temperatures ranged from 8.2 °C to 28.4 °C. Precipitation for the growth period was 1096 mm in 2011 and 1019 mm in 2012 [41].

2.2. Plant Materials

Fagus crenata is a representative deciduous broadleaf tree species in Japan and is mainly distributed in deciduous broadleaf forests of the warm-temperate zone of East Asia. *Fagus crenata* have late-successional traits. Their shoot developmental pattern is classified as flush type shoot growth [53], in which shoots are usually flushed once in the spring. Nine current-year, dormant seedlings of *F. crenata* (about 5 cm in height) were transplanted directly into the ground in each frame in March 2011. Tree seedlings were grown for two growth seasons under each of the treatment conditions described above. The maximum height of the seedlings at the end of this experiment was 132.7 cm, which was lower than the frame height.

2.3. Gas-Exchange Measurements

Light-saturated net CO₂ assimilation rates per leaf area ($A_{\text{growth-CO}_2}$) in each ambient CO₂ concentration level (at 380 $\mu\text{mol mol}^{-1}$ and 550 $\mu\text{mol mol}^{-1}$ for ambient and elevated CO₂ conditions, respectively) were measured five times in first-flush leaves during mid-May, early July, early August, mid-September, and late October of the second year of CO₂ and O₃ exposures. Leaf photosynthetic parameters at ambient (380 $\mu\text{mol mol}^{-1}$) and elevated CO₂ (550 $\mu\text{mol mol}^{-1}$) concentrations were measured in three individual seedlings per treatment combination using a portable photosynthesis system (Li-6400, Li-Cor) and a leaf chamber fluorometer (Li-6400-40, Li-Cor). Measurements were taken with the block temperature set at 27 °C and at a saturating light intensity of 1500 $\mu\text{mol m}^{-2} \text{s}^{-1}$. Light was provided by a red/blue LED array with blue light comprising 10% of the total PFD. In preliminary studies, this light intensity was sufficient to saturate A in *F. crenata*. Gas-exchange measurements were conducted from 9:00 to 15:00. Prior to these measurements, sunscreens were placed over the frames to prevent direct sunlight from illuminating the leaves.

In August 2012, A - C_i relationships of the first flush leaves were determined and used to calculate maximum rates of carboxylation at 25 °C ($V_{\text{cmax}25}$). The A - C_i curves were determined in six steps with saturating light at 1500 $\mu\text{mol m}^{-2} \text{s}^{-1}$, starting from an ambient CO₂ concentration for each treatment (380 or 550) followed by 100-, 200-, 380-, 550-, and 1000- $\mu\text{mol CO}_2 \text{ mol}^{-1}$. Measurements were taken at a block temperature of 27 °C. Maximum rates of carboxylation (V_{cmax}) were estimated using the following equation of the Farquhar-type model [55]: $A = V_{\text{cmax}} (C_c - \Gamma^*) / \{C_c + K_c \times (1 + O_i/K_o)\}$

– R_d , where C_c is the CO_2 concentration in the chloroplasts, Γ^* is the CO_2 compensation point, K_c and K_o are the Michaelis–Menten constants for carboxylation and oxygenation, O_i is the intercellular O_2 concentration, and R_d is the rate of daytime respiration. In this study, we ignored possible CO_2 diffusion limitations within leaves, and used C_i as a proxy for C_c . Values for the coefficients K_c , K_o , and Γ^* were 404.9, 278.4, and 42.75 $\mu\text{mol mol}^{-1}$, respectively, at 25 °C [56]. V_{cmax} was calculated by fitting the equation to the initial slope of the A/C_i curve ($C_i < 300$).

2.4. Chlorophyll Fluorescence Measurements

To quantitate the degree of aging-related senescence following CO_2 and O_3 treatments, we determined initial (F_0) and maximum fluorescence (F_m) values in all leaves used for the gas exchange measurements after overnight dark-adaptation using a portable fluorometer (MINI-PAM, Walz, Effeltrich, Germany). Saturating pulse of 7000 $\text{mol m}^{-2} \text{s}^{-1}$ for 1 s was used to determine F_m values. The ratio of variable to maximum fluorescence (F_v/F_m where $F_v = F_m - F_0$) represents the maximum PS II photochemical efficiency [57].

2.5. Leaf Characteristics

Leaves were collected after the measurements of F_v/F_m and leaf areas were measured using a scanner and Image J software (NIH, Bethesda, MD, USA). Dry weights of each leaf were measured after oven-drying at 70 °C and leaf mass per leaf area (LMA) was calculated for each leaf. Nitrogen concentrations of each leaf (leaf N_{mass}) were analyzed using an NC-analyzer (NT-900, SUMIKA Chem., Osaka, Japan), and N contents per leaf area (leaf N_{area}) were calculated using LMA.

2.6. Growth Measurements

In November of the second year, gas-exchange measurements were completed and all seedlings were harvested ($n = 15$, control; $n = 15$, + CO_2 ; $n = 22$, + O_3 ; $n = 21$, + CO_2 + O_3). Root systems were then excavated using an air excavation tool (Air Schop, KF Company, Sakai, Japan) to loosen soils [45]. Loosened soils were then carefully removed by hand using small stainless-steel rakes (Bonsai rake, Kikuwa, Sanjo, Niigata, Japan). Dry weights of leaves, current-year shoots, stems, and roots were determined after oven-drying to a constant weight at 70 °C.

2.7. Statistical Analysis

Significant effects of CO_2 and O_3 treatments on plant biomass, organ biomass (leaves, current-year shoots, stems and non-current-year shoots, and roots), second-flush shoot lengths, $A_{\text{growth-}\text{CO}_2}$, $g_{\text{sw-growth-}\text{CO}_2}$, C_i , leaf N_{mass} , leaf N_{area} , and LMA were identified using ANOVA with mean values from each frame ($\text{CO}_2 \times \text{O}_3$ regimen; $n = 12$). Values were averaged to calculate sample estimates for each replicate. Standardized major axis tests and routines (SMA) regression [58,59] analyses were used to examine relationships among \log_{10} -transformed whole plant and plant tissue (g plant^{-1}) biomasses using the SMATR 3.3 package [60]. Differences in elevations of SMA regressions were tested among treatments using Sidak's adjusted pair-wise tests, depending on the significance of the null hypothesis that the slopes were equal. Analyses were performed using data from all plants of each treatment group. All statistical analyses were performed using R version 3.2.3 [61].

3. Results

3.1. Photosynthesis

Net CO_2 assimilation rate responses to CO_2 and O_3 treatments varied widely with leaf age (Figure 1A, Table 1). Although $A_{\text{growth-}\text{CO}_2}$ increased following treatment with elevated CO_2 concentrations in younger leaves (May, $p = 0.088$; July, $P = 0.082$), no positive effects of elevated CO_2 were observed in older leaves (August to October). During August, $V_{\text{cmax}25}$ declined more in the + O_3 treatment group than in control plants, yet no significant effects of CO_2 and O_3 treatments

were identified (Table 1). In October, $A_{\text{growth-CO}_2}$ did not significantly decline due to elevated O_3 exposure, and predawn F_v/F_m was lower in the + O_3 treatment group than in all other groups (Table 1). Stomatal conductance ($g_{\text{sw-growth-CO}_2}$) decreased by elevated CO_2 in May ($p = 0.036$) and July ($p = 0.017$) (Figure 1B, Table 1). A tendency for effects of the O_3 were also detected only in July ($p = 0.058$). During September and October, seedlings of the + CO_2 + O_3 group tended to have the lowest $g_{\text{sw-growth-CO}_2}$ values. Finally, elevated O_3 had no effect on C_i throughout the growing season (Figure 1C).

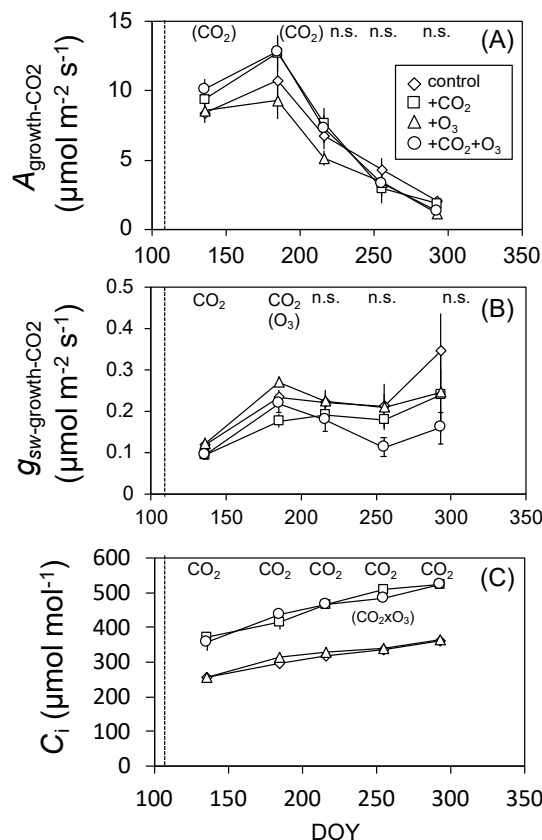


Figure 1. Seasonal changes in the light-saturated net CO_2 assimilation rate ($A_{\text{growth-CO}_2}$) (A), stomatal conductance ($g_{\text{sw-growth-CO}_2}$) (B), and intercellular CO_2 concentration (C_i) (C) in the first flush leaves of *F. crenata* seedlings grown under the CO_2 and O_3 treatment combinations at each ambient CO_2 level (380 and $550 \mu\text{mol mol}^{-1}$). Diamond: control, square: elevated CO_2 , triangle: elevated O_3 , circle: the combination of elevated CO_2 and O_3 . Dotted line shows the period of the bud break. The effects ($p < 0.05$) of CO_2 treatments, O_3 treatments, and the interaction CO_2 and O_3 on each parameter for each measurement period (five times) are indicated in the panel by CO_2 , O_3 , and $\text{CO}_2 \times \text{O}_3$, respectively. The parenthesis indicate difference at $p < 0.1$, and n.s. indicate nonsignificant ($p > 0.1$). Values are means \pm SE ($n = 3$).

3.2. Leaf Characteristics

Leaf N_{mass} of *F. crenata* seedlings was decreased by CO_2 treatment in May ($F_{1,8} = 25.8$; $p = 0.001$), and August ($F_{1,8} = 3.8$; $p = 0.088$; Figure 2A). In August, O_3 treatments also affected leaf N_{mass} ($F_{1,8} = 9.2$; $p = 0.016$). Effects of CO_2 in May ($F_{1,8} = 6.9$; $p = 0.031$) and its interactions with O_3 in July ($F_{1,8} = 4.0$; $p = 0.080$) on LMA were observed (Figure 2B). Specifically, + CO_2 + O_3 -treated seedlings had the highest LMA values among the four treatment groups in all growth periods, yet no significant effects of CO_2 and O_3 treatments were identified. Leaf N_{area} values showed interactive effects of CO_2 and O_3 treatments in September ($F_{1,8} = 7.1$; $p = 0.028$), May ($F_{1,8} = 3.8$; $p = 0.087$) and August ($F_{1,8} = 3.7$; $p = 0.091$) in addition to the effects of O_3 treatments in August (Figure 2C; $F_{1,8} = 21.5$; $p = 0.0017$).

Table 1. Light-saturated net CO₂ assimilation rate ($A_{\text{growth-CO}_2}$) and stomatal conductance ($g_{\text{sw-growth-CO}_2}$) in May and July at each ambient CO₂ level (380 and 550 $\mu\text{mol mol}^{-1}$), the maximum rate of carboxylation at 25 °C (V_{cmax25}) in August, and the maximum PS II photochemical efficiency (F_v/F_m) at predawn in October in the first flush leaves of *F. crenata* grown under ambient air (control), elevated CO₂ (+CO₂), elevated O₃ (+O₃), and the combination of elevated CO₂ and O₃ (+CO₂+O₃). Values at upper half lines are means \pm SE of three replicates for each treatment. *F* values of analysis of variance (ANOVA) to test the main effects of CO₂, O₃, and their interactions are also shown at lower half lines. Significant effects are indicated by *; $p < 0.05$, and n.s.; non-significant.

Treatments	$A_{\text{growth-CO}_2}$ ($\mu\text{mol m}^{-2} \text{s}^{-1}$)		$g_{\text{sw-growth-CO}_2}$ ($\mu\text{mol m}^{-2} \text{s}^{-1}$)		V_{cmax25} ($\mu\text{mol m}^{-2} \text{s}^{-1}$)	Predawn- F_v/F_m
	(May)	(July)	(May)	(July)	(August)	(October)
Control	8.4 \pm 0.8	10.8 \pm 1.6	0.12 \pm 0.01	0.23 \pm 0.02	30.1 \pm 3.5	0.76 \pm 0.01
+CO ₂	9.4 \pm 0.3	12.7 \pm 1.3	0.09 \pm 0.01	0.18 \pm 0.02	23.0 \pm 2.1	0.78 \pm 0.01
+O ₃	8.6 \pm 0.6	9.3 \pm 1.4	0.12 \pm 0.01	0.27 \pm 0.01	21.9 \pm 2.0	0.65 \pm 0.04
+CO ₂ +O ₃	10.1 \pm 0.7	12.9 \pm 1.1	0.09 \pm 0.01	0.22 \pm 0.02	22.2 \pm 2.8	0.72 \pm 0.01
Effect						
CO ₂ ($F_{1,8}$)	3.7 n.s.	4.0 n.s.	6.34 *	8.94 *	1.65 n.s.	0.08 n.s.
O ₃ ($F_{1,8}$)	0.5 n.s.	0.2 n.s.	0.05 n.s.	4.90 n.s.	2.86 n.s.	2.97 n.s.
CO ₂ \times O ₃ ($F_{1,8}$)	0.2 n.s.	0.3 n.s.	0.00 n.s.	0.01 n.s.	1.93 n.s.	0.03 n.s.

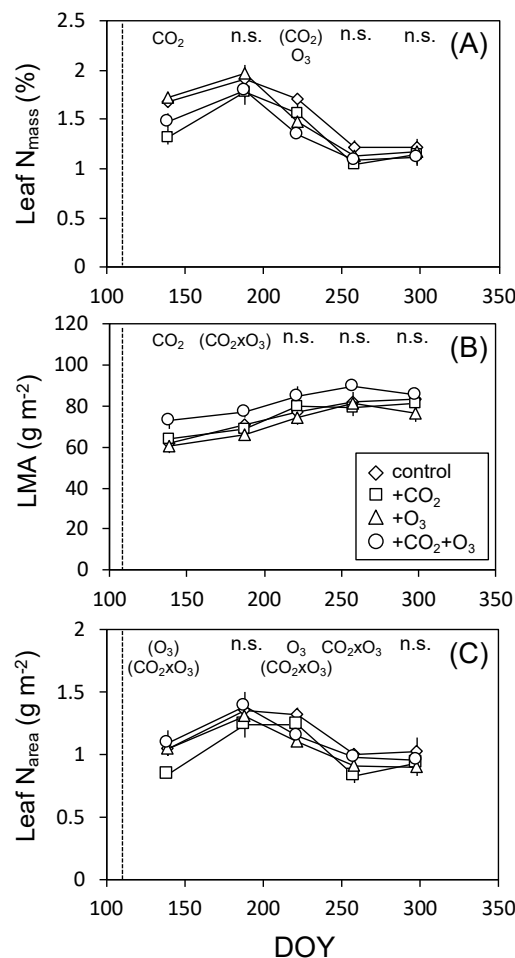


Figure 2. Seasonal change in the leaf N concentration (leaf N_{mass}) (A), leaf mass per area (LMA) (B), and area-based leaf N content (leaf N_{area}) (C) in the first flush leaves of *F. crenata* seedlings grown under the CO₂ and O₃ treatment combinations at each ambient CO₂ level (380 and 550 $\mu\text{mol mol}^{-1}$). The format of these figures is the same as in Figure 1.

3.3. Plant Biomass

Elevated CO₂ concentrations had positive effects on the whole plant biomasses (Total) of *F. crenata* seedlings (Table 2; $p = 0.033$). Seedlings of the +CO₂+O₃ treatment group tended to exhibit the largest average plant biomass among the four treatment groups ($p = 0.037$, in one-way ANOVA). Though no significant effects of CO₂ and O₃ treatments were identified in dry matter distribution, elevated CO₂ concentrations showed a tendency to decrease RWR ($p = 0.078$) and increase aboveground biomass to root ratio (S:R ratio) ($p = 0.066$), and leaf to root ratio (L:R ratio) tended to increase by elevated O₃ treatment ($p = 0.065$) (Table 3). All treatment groups included some seedlings that had a second flush leaf production. Yet only following +CO₂+O₃ treatments did all plants produce second-flush leaves (77.8% ± 14.7%, Control; 68.9% ± 17.4%, +CO₂; 81.9% ± 10.8%, +O₃; and 100%, +CO₂+O₃; these values indicated mean ± SE). Lengths of second-flush shoots (mean ± SE) were also affected by CO₂ concentrations ($p = 0.030$) and were 31.4 ± 12.4 cm in control plants, 51.3 ± 5.9 cm in +CO₂ treated plants; 32.7 ± 2.9 cm in +O₃ treated plants, and 49.8 ± 1.1 cm in +CO₂+O₃ treated plants.

Table 2. Dry mass of plant tissues (whole plant; Total, leaf weight; Leaf, current shoot weight; Current shoot; stem and shoot weight; Stem and shoot, root weight; Root) of the seedling of *F. crenata* grown under ambient air (control), elevated CO₂ (+CO₂), elevated O₃ (+O₃), and the combination of elevated CO₂ and O₃ (+CO₂+O₃). Values at upper half lines are means ± SE of three replicates for each treatment. *F* values of analysis of variance (ANOVA) to test the main effects of CO₂, O₃, and their interactions are also shown at lower half lines. Significant effects are indicated by *, $p < 0.05$, and n.s.; non-significant.

Treatments	Total	Leaf	Current Shoot	Stem and Shoot	Root
Control	43.3 ± 9.6	5.5 ± 1.5	8.8 ± 3.2	8.7 ± 1.3	20.3 ± 3.7
+CO ₂	45.4 ± 6.4	5.3 ± 1.3	10.0 ± 2.6	10.2 ± 1.6	19.9 ± 2.2
+O ₃	39.2 ± 0.7	5.4 ± 0.5	6.9 ± 0.3	8.9 ± 1.2	18.0 ± 0.9
+CO ₂ +O ₃	67.1 ± 1.3	9.2 ± 0.4	16.4 ± 0.6	15.1 ± 1.3	26.4 ± 0.8
Effect					
CO ₂ (F _{1,8})	6.6 *	3.1 n.s.	6.5 *	7.8 *	3.2 n.s.
O ₃ (F _{1,8})	2.3 n.s.	3.4 n.s.	1.2 n.s.	3.5 n.s.	0.9 n.s.
CO ₂ × O ₃ (F _{1,8})	4.9 n.s.	3.8 n.s.	3.9 n.s.	2.9 n.s.	3.8 n.s.

Table 3. Dry matter distribution (leaf weight ratio; LWR, current shoot weight ratio; CSWR, stem and shoot weight ratio; SWR, root weight ratio; RWR, and aboveground biomass to root ratio; S:R ratio, leaf to root ratio; L:R ratio) of the seedling of *F. crenata* grown under ambient air (control), elevated CO₂ (+CO₂), elevated O₃ (+O₃), and the combination of elevated CO₂ and O₃ (+CO₂+O₃). Values at upper half lines are means ± SE of three replicates for each treatment. *F* values of analysis of variance (ANOVA) to test the main effects of CO₂, O₃, and their interactions are also shown at lower half lines. There is no significant effect in all parameters, which indicated by n.s.; non-significant.

Treatments	LWR	CSWR	SWR	RWR	S:R Ratio	L:R Ratio
Control	0.12 ± 0.01	0.19 ± 0.03	0.21 ± 0.02	0.48 ± 0.02	1.12 ± 0.09	0.26 ± 0.04
+CO ₂	0.12 ± 0.02	0.21 ± 0.03	0.23 ± 0.03	0.44 ± 0.02	1.30 ± 0.11	0.26 ± 0.04
+O ₃	0.14 ± 0.01	0.18 ± 0.00	0.23 ± 0.03	0.45 ± 0.02	1.25 ± 0.13	0.30 ± 0.02
+CO ₂ +O ₃	0.14 ± 0.01	0.24 ± 0.01	0.21 ± 0.01	0.41 ± 0.01	1.50 ± 0.06	0.35 ± 0.02
Effect						
CO ₂ (F _{1,8})	0.01 n.s.	2.84 n.s.	0.03 n.s.	4.07 n.s.	4.52 n.s.	0.82 n.s.
O ₃ (F _{1,8})	3.37 n.s.	0.09 n.s.	0.01 n.s.	2.24 n.s.	2.65 n.s.	4.57 n.s.
CO ₂ × O ₃ (F _{1,8})	0.05 n.s.	0.82 n.s.	0.65 n.s.	0.08 n.s.	0.18 n.s.	0.91 n.s.

3.4. Biomass Allocation

In our allometric assessments of relationships between whole plant weights and root weights, regression slopes did not differ among treatments ($p = 0.231$; Figure 3A, Table 4). In case the common

slopes of 1.015 (0.947–1.091; $\pm 95\%$ confidence intervals (CI)) were used, magnitudes of relationships differed significantly between treatment groups ($p = 0.0002$). Specifically, seedlings from the +CO₂+O₃ treatment group had smaller elevations than those of the control and the +O₃ treatment groups. Allometric assessments of root and leaf weights also gave slopes that did not differ between treatments ($p = 0.114$; Figure 3B, Table 4). At common slopes of 0.979 (0.831–1.153; $\pm 95\%$ CI), magnitudes of these relationships differed significantly between treatment groups ($p = 0.0087$). The +CO₂+O₃ treatment led to greater elevation than that observed in control and the +CO₂ treatment group. In allometric assessments, the regression slopes in relationships between whole plant and leaf weights ($p = 0.013$) and between whole plant and shoot weights ($p = 0.032$) differed significantly between treatments. The slopes ($p = 0.635$) and magnitudes ($p = 0.725$) of the allometric relationships between whole plant and stem weights did not differ.

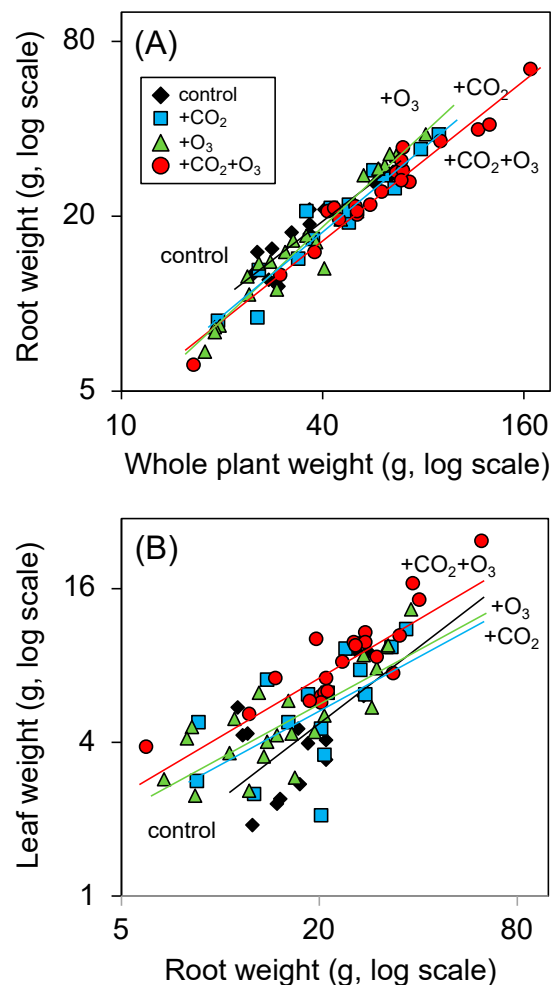


Figure 3. Allometric relationships between whole plant weight and root weight (A) and between root weight and leaf weight (B) of *F. crenata* seedlings. Allometric equations analyzed by using an R package, smart 3 (SMA analysis), are listed in Table 4. Diamond (black): control, square (blue): elevated CO₂, triangle (green): elevated O₃, circle (red): the combination of elevated CO₂ and O₃. Each colored line shows regression line for each treatment.

Table 4. Standardized major axis (SMA) regression slopes and their confidence intervals for log-log transformed relationships between whole plant weight and root weight (Figure 3A) and between root weight and leaf weight (Figure 3B) of *F. crenata* seedlings grown under ambient air (control), elevated CO₂ (+CO₂), elevated O₃ (+O₃), and the combination of elevated CO₂ and O₃ (+CO₂+O₃). Values of coefficients of determination (*r*²) and significant values (*p*) of each bivariate relationship are shown. 95% confidence intervals (CI) of SMA slopes and *y*-axis intercepts are exhibited. In cases where SMA tests for common slopes revealed no significant differences between treatments, common slopes are used. The differences in elevations of the SMA regressions are tested among treatments using Sidak’s adjusted pair-wise test, depending on the significance of the null hypothesis that the slopes are equal. Where there is a significant difference in elevation of the common-slope SMA regressions, values for the *y*-axis intercept (elevation) are provided. Different letters in pairwise comparison are significantly different, with a *p* < 0.05 under the slopes are equal. Where appropriate, significant shifts along a common slope are indicated. The format of table is referred that in Atkin et al. [59].

Response	Whole Plant Weight				Leaf Weight			
Bivariate	Root Weight				Root Weight			
H0 NO. 1: no difference in slope (<i>p</i> -value)								
	0.231				0.114			
Treatment	Control	+CO ₂	+O ₃	+CO ₂ +O ₃	Control	+CO ₂	+O ₃	+CO ₂ +O ₃
<i>n</i>	15	15	22	21	15	15	22	21
<i>r</i> ²	0.859	0.917	0.946	0.952	0.393	0.367	0.626	0.751
<i>p</i> -value	<0.0001	<0.0001	<0.0001	<0.0001	0.012	0.017	<0.0001	<0.0001
Slope	0.961	1.018	1.107	0.952	1.579	1.152	0.891	0.887
Slope CI_high	1.202	1.208	1.233	1.058	2.480	1.826	1.180	1.125
Slope CI_Low	0.768	0.858	0.993	0.857	1.006	0.727	0.672	0.700
Intercept	−0.257	−0.392	−0.509	−0.315	−0.592	−0.766	−0.385	−0.304
H0 NO. 2: no difference in elevation (<i>p</i> -value)								
	0.0002				0.009			
Intercepts for a common slope	−0.343	−0.387	−0.368	−0.427	−0.592	−0.544	−0.492	−0.431
Pairwise comparison (where relationship significant)								
	a	ab	a	b	b	b	ab	a
H0 NO. 3: no difference in ‘shift’ (<i>p</i> -value)								
	0.015				0.002			

4. Discussion

The present screen-aided FACE experiment demonstrated that the growth of *F. crenata* was enhanced by O₃ exposure under elevated CO₂, but not under ambient CO₂ (Table 2). The increased biomass of *F. crenata* seedling under +CO₂+O₃ treatment might reflect (1) an alleviation of the negative effect of O₃ on photosynthetic activity (leaf level response; Figure 1, Table 1), and (2) an increase in biomass allocation into leaves at the expense of root growth (plant-level responses; Figure 3, Table 4). The incremental increase in the biomass of *F. crenata* under +CO₂+O₃ was less than those reported in two *Quercus* species grown under elevated CO₂ and O₃ [45]. Watanabe et al. [50] also reported incremental increases in plant biomass of *F. crenata* in open top chamber (OTC) experiments with elevated CO₂ and O₃ concentrations. Our field experiment confirmed that elevated CO₂ ameliorated the negative effects of elevated O₃ in *F. crenata* trees, which are highly susceptible to increased O₃ levels.

The positive effects by elevated CO₂ on the whole plant biomasses of *F. crenata* seedlings were shown in this relatively short-term experiment (Table 2). It is obvious that the responses to elevated CO₂ are dependent on the duration of exposure. Agathokleous et al., [62] reported that 11 years of exposure of CO₂ in the FACE system, established in the nursery of Hokkaido University (Sapporo, Japan), induced rhizomorphogenesis, with a massive production of fine roots, especially in the phosphorus-limited volcanic ash soils, but not in the brown forest soils. The observations from different systems and experimental setups suggest that the effect of elevated CO₂ on *F. crenata* would be dependent on soil conditions.

Fagus crenata seedlings grown under +CO₂+O₃ showed the lowest $g_{sw-growth-CO_2}$ values among the all treatment combinations in the later growing season (Figure 1B), suggesting a reduction in O₃ uptake under the conditions of +CO₂+O₃. Hence, as a leaf level photosynthetic response, the negative effects of O₃ on $A_{growth-CO_2}$ of *F. crenata* might be alleviated by higher CO₂ levels due to reduced O₃ uptake (Figure 1A). Elevated CO₂-induced decreases in stomatal conductance were also reported in *F. crenata* and other species under high CO₂ and O₃ levels [50,51]. Compensation for O₃-induced reductions in area-based CO₂ uptake rates may partly reflect lowered O₃ uptake rates due to stomatal narrowing in response to elevated CO₂ [21,52]. Several studies on broadleaf tree species have reported similar effects of elevated CO₂ alleviating O₃-related foliar injury [21,51].

Plants grown under +CO₂+O₃ showed the highest LMA throughout growth season (Figure 2B). Plants with higher LMA reportedly have high tolerance to elevated O₃ [3,15,27], which may also decrease concentrations of total nonstructural carbohydrates (TNC; soluble sugar and starch) and alter their distributions among plant tissues [24]. On contrast, TNC is usually increased in leaves under elevated CO₂ conditions, which enhance LMA [63]. Ozone damages leaf cells and thus adversely affects plant production, reduces photosynthetic rates, and demands increased resource allocation to detoxify and repair leaves [6]. Lindroth [8] suggested that enriched in CO₂ concentrations can increase carbon availability for the production of defense compounds pathways that are upregulated in response to O₃. Matsumura et al. [51] and Karonen et al. [64] showed that condensed tannins are present at significantly higher levels in seedlings of *F. crenata* after combined treatments with high CO₂ and O₃ levels. The changes in TNC and these defense compounds may contribute to increased LMA in *F. crenata* under combined increases in CO₂ and O₃ levels, yet we did not determine both of them in the present study.

Elevated O₃ can impair C metabolism and decrease C stocks [24], and several studies indicate decreases in biomass allocation into roots [26]. In the plant-level responses of *F. crenata* seedlings shown herein, allometric relationships between whole plant weight and root weight, and between roots and leaves were modified by +CO₂+O₃ treatments (Figure 3, Table 4). This suggests that *F. crenata* seedlings grown under the +CO₂+O₃ allocated larger amounts of biomass to aboveground tissues than belowground tissues, resulting in higher S:R ratio and L:R ratio, and in lower RWR compared with other treatments (Table 3). Reduced C allocation into root has also been demonstrated in young [16,30,65] and mature trees of *Fagus* species under conditions of elevated O₃ [19]. However, in mature *Fagus* species, different responses to elevated O₃ were also observed, such as stimulation of root growth [66,67] and no changes in carbon allocation into belowground tissues [68]. In addition, soil nutrient supply mitigated the negative impacts of O₃ on biomass allocation in *F. crenata* seedlings [69,70].

In our study, all *F. crenata* seedlings grown under +CO₂+O₃ produced second-flush shoots. In addition, +CO₂+O₃ led to the greatest average length of the secondary shoots among the treatment combinations, although *F. crenata* is a determinate tree species that usually flushes shoots once a year. Watanabe et al. [50] also showed similar growth responses with enhanced second flushes of *F. crenata* under elevated CO₂ and O₃ in OTC experiments. This suggests that the greater investment of carbohydrate due to the higher photosynthetic rate in first flush leaves contributed to the increase in new leaf emergence. Kolb and Matyssek [71] similarly showed that plants with more determinate growth habits tend to respond to O₃ exposure by reducing carbon allocation to root growth, in favor of maintaining older leaves and supporting new leaf flushes. Sitch et al. [20] also suggested that translocation patterns to different plant organs might depend as much on sink activities as well as source strengths. In our study, the balance between higher source activity ($A_{growth-CO_2}$) due to increased CO₂ concentration, and higher sink strength for detoxification and repair of leaves following O₃ exposure, might be responsible for the changes in allometric relationships between roots and leaves. Conversely, lower $A_{growth-CO_2}$ and smaller numbers of second-flush leaves in *F. crenata* seedlings of the +O₃ treatment group may underlie the comparatively unclear changes in biomass allocation.

We observed declines in F_v/F_m ratios of *F. crenata* under elevated O₃ later in the growth season (Table 1), suggesting that autumn leaf senescence was accelerated by O₃ exposure. Watanabe et al. [72]

performed FACE experiments and showed ozone-induced reductions in light-saturated photosynthetic rates in upper canopy leaves of *F. crenata* during August and October, but not during July. Grams et al. [21] also reported marked declines in photosynthetic rate responses to O₃ in *Fagus sylvatica* during the late season. In addition, even current ambient atmospheric O₃ levels have accelerated autumn senescence in a forest of *F. crenata* in the northern part of Japan [49]. These dynamic interactions between plant development, carbon allocation, and O₃ exposure are important for understanding future impacts of ozone on forest ecosystems [6]. The results of our screen-aided free-air O₃ and CO₂ exposure experiments in the field may contribute to predictions of tree responses to future climate change.

Since both CO₂ and O₃ are categorized global-warming-gases, along with increased O₃ and CO₂ concentrations, ambient air temperature may increase in the future. However, our study did not treat air temperature, and the air temperature in each frame was not affected by CO₂ and O₃ treatments. Hence, this study focused on the effects of increased CO₂ and O₃ without consideration of temperature.

5. Conclusions

Screen-aided FACE experiments demonstrated that the growth of *Fagus crenata* seedlings was enhanced by combined increases in O₃ and CO₂ concentrations, which was related to the modified C allocation between roots and leaves (plant-level responses), and the alleviation of O₃ impact on net CO₂ assimilation by elevated CO₂ (leaf level responses). It is noteworthy that the extent of growth enhancement was not as large as that reported in *Quercus* species [45]. The intrinsic lower plasticity of leaf expansion pattern in *F. crenata* would affect the growth responses to future combinations of increased O₃ and CO₂ levels.

Author Contributions: H.T. and M.K. designed the study. H.T., M.K., H.H., K.Y., S.K., and M.K. collected the photosynthetic data, performed the analysis, and hence equally contributed to this study. All authors also discussed the results and commented on the manuscript.

Funding: This study was supported in part by the project on “Technology development for circulatory food production systems responsive to climate change” conducted by the Ministry of Agriculture, Forestry and Fisheries, Japan, the Grant-in-Aid for Scientific Research (B) (No. 25292092) and JSPS KAKENHI Grant Number JP17H03839.

Acknowledgments: We thank K Sakai and K. Arai for assistance with measurements. We also thank Morikawa for his valuable suggestions concerning the present study.

Conflicts of Interest: The authors declare no conflict of interest.

References

1. Chen, Z.; Shang, H.; Cao, J.; Yu, H. Effects of ambient ozone concentrations on contents of nonstructural carbohydrates in *Phoebe bournei* and *Pinus massoniana* seedlings in subtropical China. *Water Air Soil Pollut.* **2015**, *226*, 310–317. [[CrossRef](#)]
2. Dentener, F.; Stevenson, D.; Ellingsen, K.; van Noije, T.; Schultz, M.; Amann, M.; Atherton, C.; Bell, N.; Bergmann, D.; Bey, I.; et al. The global atmospheric environment for the next generation. *Environ. Sci. Technol.* **2006**, *40*, 3586–3594. [[CrossRef](#)] [[PubMed](#)]
3. Feng, Z.; Büker, P.; Pleijel, H.; Emberson, L.; Karlsson, P.E.; Uddling, J. A unifying explanation for variation in ozone sensitivity among woody plants. *Glob. Chang. Biol.* **2018**, *24*, 78–84. [[CrossRef](#)] [[PubMed](#)]
4. IPCC. *Climate Change 2013: The Physical Science Basis*; Stocker, T.F., Qin, D., Plattner, G.-K., Tignor, M., Allen, S.K., Boschung, J., Nauels, A., Xia, Y., Bex, B., Midgley, P.M., Eds.; Contribution of Working Group I to the Fifth Assessment Report of the Intergovernmental Panel on Climate Change; Cambridge University Press: Cambridge, UK, 2013.
5. Monks, P.S.; Archibald, A.T.; Colette, A.; Cooper, O.; Coyle, M.; Derwent, R.; Fowler, D.; Granier, C.; Law, K.S.; Mills, G.E.; et al. Tropospheric ozone and its precursors from the urban to the global scale from air quality to short-lived climate forcer. *Atmos. Chem. Phys.* **2015**, *15*, 8889–8973. [[CrossRef](#)]
6. Ashmore, M.R. Assessing the future global impacts of ozone on vegetation. *Plant Cell Environ.* **2005**, *28*, 949–964. [[CrossRef](#)]

7. Karnosky, D.F.; Pregitzer, K.S.; Zak, D.R.; Kubiske, M.E.; Hendrey, G.R.; Weinstein, D.; Nosal, M.; Percy, K.E. Scaling ozone responses of forest trees to the ecosystem level in a changing climate. *Plant Cell Environ.* **2005**, *28*, 965–981. [[CrossRef](#)]
8. Lindroth, R.L. Atmospheric change, plant secondary metabolites and ecological interactions. In *The Ecology of Plant Secondary Metabolites: From Genes to Global Progresses*; Iason, G.R., Dick, M., Hartley, S.E., Eds.; Cambridge University Press: Cambridge, UK, 2012; pp. 120–153.
9. Wittig, V.E.; Ainsworth, E.A.; Naidu, S.L.; Karnosky, D.F.; Long, S.P. Quantifying the impact of current and future tropospheric ozone on tree biomass, growth, physiology and biochemistry: A quantitative meta-analysis. *Glob. Chang. Biol.* **2009**, *15*, 396–424. [[CrossRef](#)]
10. Ainsworth, E.A.; Davey, P.A.; Hymus, G.J.; Osborne, C.P.; Roger, A.; Blum, H.; Nösberger, J.; Long, S.P. Is stimulation of leaf photosynthesis by elevated carbon dioxide concentration maintained in the long term? A test with *Lolium perenne* grow for 10 years at two nitrogen fertilization levels under Free Air CO₂ Enrichment (FACE). *Plant Cell Environ.* **2003**, *26*, 705–714. [[CrossRef](#)]
11. Davey, P.A.; Olcer, H.; Zakhleniuk, O.; Bernacchi, C.J.; Calfapietra, C.; Long, S.P.; Raines, C.A. Can fast-growing plantation trees escape biochemical down-regulation of photosynthesis when grown throughout their complete production cycle in the open air under elevated carbon dioxide? *Plant Cell Environ.* **2006**, *29*, 1235–1244. [[CrossRef](#)]
12. Zak, D.R.; Pregitzer, K.S.; Kubiske, M.E.; Burton, A.J. Forest productivity under elevated CO₂ and O₃: Positive feedbacks to soil N cycling sustain decade-long net primary productivity enhancement by CO₂. *Ecol. Lett.* **2011**, *14*, 1220–1226. [[CrossRef](#)]
13. Norby, R.J.; Warren, J.M.; Iversen, C.M.; Medlyn, B.E.; McMurtrie, R.E. CO₂ enhancement of forest productivity constrained by limited nitrogen availability. *Proc. Natl. Acad. Sci. USA* **2010**, *107*, 19368–19373. [[CrossRef](#)] [[PubMed](#)]
14. Sigurdsson, B.D.; Medhurst, J.L.; Wallin, G.; Eggertsson, O.; Linder, S. Growth of mature boreal Norway spruce was not affected by elevated [CO₂] and/or air temperature unless nutrient availability was improved. *Tree Physiol.* **2013**, *33*, 1192–1205. [[CrossRef](#)] [[PubMed](#)]
15. Li, P.; Calatayud, V.; Gao, F.; Uddling, J.; Feng, Z. Differences in ozone sensitivity among woody species are related to leaf morphology and antioxidant levels. *Tree Physiol.* **2016**, *36*, 1105–1116. [[CrossRef](#)] [[PubMed](#)]
16. Matyssek, R.; Sandermann, H. Impact of ozone on trees: An ecophysiological perspective. *Prog. Bot.* **2003**, *64*, 349–404.
17. Matyssek, R.; Wieser, G.; Ceulemans, R.; Rennenberg, H.; Pretzsch, H.; Haberer, K.; Low, M.; Nunn, A.J.; Werner, H.; Wipfler, P.; et al. Enhanced ozone strongly reduces carbon sink strength of adult beech (*Fagus sylvatica*)-Resume from the free-air fumigation study at Kranzberg forest. *Environ. Pollut.* **2010**, *158*, 2527–2532. [[CrossRef](#)] [[PubMed](#)]
18. Pretzsch, H.; Dieler, J.; Matyssek, R.; Wipfler, P. Tree and stand growth of mature Norway spruce and European beech under long-term ozone fumigation. *Environ. Pollut.* **2010**, *158*, 1061–1070. [[CrossRef](#)]
19. Ritter, W.; Andersen, C.P.; Matyssek, R.; Grams, T.E.E. Carbon flux to woody tissues in a beech/spruce forest during summer and in response to chronic O₃ exposure. *Biogeosciences* **2011**, *8*, 3127–3138. [[CrossRef](#)]
20. Sitch, S.; Cox, P.M.; Collins, W.J.; Huntingford, C. Indirect radiative forcing of climate change through ozone effects on the land-carbon sink. *Nature* **2007**, *448*, 791–795. [[CrossRef](#)] [[PubMed](#)]
21. Grams, T.E.E.; Anegg, S.; Haberle, K.; Langebartlet, C.; Matyssek, R. Interactions of chronic exposure to elevated CO₂ and O₃ level in the photosynthetic light and dark reactions of European beech (*Fagus sylvatica*). *New Phytol.* **1999**, *144*, 95–107. [[CrossRef](#)]
22. Percy, K.E.; Nosal, M.; Heilman, W.; Dann, T.; Sobre, J.; Legge, A.H.; Karnosky, D.F. New exposure-based metric approach for evaluating O₃ risk to North American aspen forests. *Environ. Pollut.* **2007**, *147*, 554–566. [[CrossRef](#)]
23. Volk, M.; Bungener, P.; Contat, F.; Montani, M.; Fuhrer, J. Grassland yield declined by a quarter in 5 years of free-air ozone fumigation. *Glob. Chang. Biol.* **2006**, *12*, 74–83. [[CrossRef](#)]
24. Cao, J.; Chen, Z.; Yu, H.; Shang, H. Differential responses in non-structural carbohydrates of *Machilus ichangensis* Rehd. et Wils. and *Taxus wallichiana* Zucc. Var. *chinensis* (Pilg.) florin seedlings to elevated Ozone. *Forests* **2017**, *8*, 323–334.

25. Chen, Z.; Cao, J.; Yu, H.; Shang, H. Effects of elevated ozone levels on photosynthesis, biomass and non-structural carbohydrates of *Phoebe bournei* and *Phoebe zhennan* in subtropical China. *Front. Plant Sci.* **2018**, *9*, 1764–1772. [[CrossRef](#)] [[PubMed](#)]
26. Agathokleous, E.; Saitanis, C.J.; Wang, X.; Watanabe, M.; Koike, T. A review study on past 40 years of research on effects of tropospheric O₃ on belowground structure, functioning, and processes of trees: A linkage with potential ecological implications. *Water Air Soil Pollut.* **2016**, *227*, 33. [[CrossRef](#)]
27. Feng, Z.; Li, P. Effects of ozone on Chinese trees. In *Air Pollution Impacts on Plants in East Asia*; Springer Japan: Tokyo, Japan, 2017; pp. 195–219.
28. Karlsson, P.E.; Uddling, J.; Skärby, L.; Wallin, G.; Sell-dén, G. Impact of ozone on the growth of birch (*Betula pendula*) saplings. *Environ. Pollut.* **2003**, *124*, 485–495. [[CrossRef](#)]
29. Oksanen, E.; Rousi, M. Differences of *Betula* origins in ozone sensitivity based on open-field experiment over two growing seasons. *Can. J. For. Res.* **2001**, *31*, 804–811. [[CrossRef](#)]
30. Winkler, B.; Fleischmann, F.; Gayler, S.; Scherb, H.; Matyssek, R.; Grams, T.E.E. Do chronic aboveground O₃ exposure and belowground pathogen stress affect growth and belowground biomass partitioning of juvenile beech trees (*Fagus sylvatica* L.)? *Plant Soil* **2009**, *323*, 31–44. [[CrossRef](#)]
31. Ainsworth, E.A. Understanding and improving global crop response to ozone pollution. *Plant J.* **2017**, *90*, 886–897. [[CrossRef](#)] [[PubMed](#)]
32. Li, P.; DeMarco, A.; Feng, Z.Z.; Anav, A.; Zhou, D.J.; Paoletti, E. Nationwide ground-level ozone measurements in China suggest serious risks to forests. *Environ. Pollut.* **2018**, *237*, 803–813. [[CrossRef](#)]
33. King, J.S.; Liu, L.; Aspinwall, M.J. Tree and forest responses to interacting elevated atmospheric CO₂ and tropospheric O₃: A synthesis of experimental evidence. In *Climate Change, Air Pollution and Global Challenges: Understanding Solutions from Forest Research*; Matyssek, R., Clarke, N., Cudlin, P., Mikkelsen, T.N., Tuovinen, J.-P., Wieser, G., Paoletti, E., Eds.; Elsevier Physical Sciences Series; Elsevier: San Diego, CA, USA, 2013; Volume 13, pp. 179–208.
34. Feng, Z.Z.; Tang, H.Y.; Uddling, J.; Pleijel, H.; Kobayashi, K.; Zhu, J.G.; Oue, H.; Guo, W.S. A stomatal ozone flux-response relationship to assess ozone-induced yield loss of winter wheat in subtropical China. *Environ. Pollut.* **2012**, *164*, 16–23. [[CrossRef](#)]
35. Hoshika, Y.; Katata, G.; Deushi, M.; Watanabe, M.; Koike, T.; Paoletti, E. Ozone-induced stomatal sluggishness changes carbon and water balance of temperate deciduous forests. *Sci. Rep.* **2015**, *5*, 9871. [[CrossRef](#)] [[PubMed](#)]
36. Bader, M.K.F.; Leuzinger, S.; Sonja, G.; Keel, S.G.; Rolf, T.W.; Siegwolf, R.T.W.; Hagedorn, F.; Schleppei, P.; Körner, C. Central European hardwood trees in a high-CO₂ future: Synthesis of an 8-year forest canopy CO₂ enrichment project. *J. Ecol.* **2013**, *101*, 1509–1519. [[CrossRef](#)]
37. Knepp, R.G.; Hamilton, J.G.; Mohan, J.E.; Zangerl, A.R.; Berenbaum, M.R.; DeLucia, E.H. Elevated CO₂ reduces leaf damage by insect herbivores in a forest community. *New Phytol.* **2005**, *167*, 207–218. [[CrossRef](#)] [[PubMed](#)]
38. Koike, T.; Watanabe, M.; Watanabe, Y.; Agathokleous, E.; Eguchi, N.; Takagi, K.; Satoh, F.; Kitaoka, S.; Funada, R. Ecophysiology of deciduous trees native to northeast Asia grown under FACE (Free Air CO₂ Enrichment). *J. Agric. Meteorol.* **2015**, *71*, 174–184. [[CrossRef](#)]
39. Norby, R.J.; Zak, D.R. Ecological lessons from free-air CO₂ enrichment (FACE) experiments. *Annu. Rev. Ecol. Evol. Syst.* **2011**, *42*, 181–203. [[CrossRef](#)]
40. Matyssek, R.; Kozovits, A.R.; Wieser, G.; King, J.; Rennenberg, H. Woody-plant ecosystems under climate change and air pollution-response consistencies across zonobiomes? *Tree Physiol.* **2017**, *37*, 706–732. [[CrossRef](#)]
41. Hiraoka, Y.; Iki, T.; Nose, M.; Tobita, H.; Tazaki, K.; Watanabe, A.; Fujisawa, I.; Kitao, M. Species characteristics and intraspecific variation in growth and photosynthesis of *Cryptomeria japonica* under elevated O₃ and CO₂. *Tree Physiol.* **2017**, *37*, 1–11. [[CrossRef](#)]
42. Hoshika, Y.; Watanabe, M.; Inada, N.; Koike, T. Ozone-induced stomatal sluggishness develops progressively in Siebold's beech (*Fagus crenata*). *Environ. Pollut.* **2012**, *166*, 152–156. [[CrossRef](#)]
43. Koike, T.; Kawaguchi, K.; Hoshika, Y.; Kita, K.; Watanabe, M.; Mao, Q.; Inada, N. Growth and photosynthetic responses of cuttings of a hybrid larch (*Larix gmelinii* var. *japonica* x *L. kaempferi*) to elevated ozone and/or carbon dioxide. *Asian J. Atmos. Environ.* **2012**, *6*, 104–110.

44. Kitao, M.; Tobita, H.; Kitaoka, S.; Harayama, H.; Yazaki, K.; Komatsu, M.; Agathokleous, E.; Koike, T. Light Energy Partitioning under Various Environmental Stresses Combined with Elevated CO₂ in Three Deciduous Broadleaf Tree Species in Japan. *Climate* **2019**, *7*, 79. [CrossRef]
45. Kitao, M.; Komatsu, M.; Yazaki, K.; Kitaoka, S.; Tobita, H. Growth overcompensation against O₃ exposure in two Japanese oak species, *Quercus mongolica* var. *crispula* and *Quercus serrata*, grown under elevated CO₂. *Environ. Pollut.* **2015**, *206*, 133–141. [PubMed]
46. Watanabe, M.; Yamaguchi, M.U.; Koike, T.; Izuta, T. Effects of ozone on Japanese trees. In *Air Pollution Impacts on Plants in East Asia*; Springer Japan: Tokyo, Japan, 2017; pp. 73–100.
47. Yamaguchi, M.; Watanabe, M.; Matsumura, H.; Kohno, Y.; Izuta, T. Experimental studies on the effects of ozone on growth and photosynthetic activity of Japanese forest tree species. *Asian J. Atmos. Environ.* **2011**, *5*, 65–78. [CrossRef]
48. Nakashizuka, T.; Iida, S. Composition, dynamics and disturbance regime of temperate deciduous forests in Monsoon Asia. *Vegetation* **1995**, *121*, 23–30. [CrossRef]
49. Kitao, M.; Yasuda, Y.; Kominami, Y.; Yamanoi, K.; Komatsu, M.; Miyama, T.; Mizoguchi, Y.; Kitaoka, S.; Yazaki, K.; Tobita, H.; et al. Increased phytotoxic O₃ dose accelerates autumn senescence in an O₃-sensitive beech forest even under the present-level O₃. *Sci. Rep.* **2016**, *6*, 32549. [CrossRef]
50. Watanabe, M.; Yamaguchi, M.U.; Koike, T.; Izuta, T. Growth and photosynthetic response of *Fagus crenata* seedlings to ozone and/or elevated carbon dioxide. *Landsc. Ecol. Eng.* **2010**, *6*, 181–190. [CrossRef]
51. Matsumura, H.; Mikami, C.; Sakai, Y.; Murayama, K.; Izuta, T.; Yonekura, T.; Miwa, M.; Kohno, Y. Impact of elevated O₃ and/or CO₂ on growth of *Betula platyphylla*, *Betula ermanii*, *Fagus crenata*, *Pinus densiflora* and *Cryptomeria japonica* seedlings. *J. Agric. Meteorol.* **2005**, *60*, 1121–1124. [CrossRef]
52. Watanabe, M.; Hoshika, Y.; Koike, T.; Izuta, T. Combined effects of ozone and other environmental factors on Japanese trees. In *Air Pollution Impacts on Plants in East Asia*; Springer Japan: Tokyo, Japan, 2017; pp. 101–110.
53. Kikuzawa, K. Leaf survival of woody plant in deciduous broad-leaved forests. 1. Tall trees. *Can. J. Bot.* **1983**, *61*, 2133–2139. [CrossRef]
54. Erbs, M.; Fangmeier, A. A chamberless field exposure system for ozone enrichment of short vegetation. *Environ. Pollut.* **2005**, *133*, 91–102. [CrossRef]
55. Farquhar, G.D.; von Caemmerer, S.; Berry, J.A. A biochemical model of photosynthetic acclimation in leaves of C₃ species. *Planta* **1980**, *149*, 78–90. [CrossRef]
56. Bernacchi, C.J.; Singsaas, E.L.; Pimentel, C.; Portis, A.R.; Long, S.P. Improved temperature response functions for models of Rubisco-limited photosynthesis. *Plant Cell Environ.* **2001**, *24*, 253–259. [CrossRef]
57. Schreiber, U.; Bilger, W.; Neubauer, C. Chlorophyll fluorescence as a noninvasive indicator for rapid assessment of in vivo photosynthesis. In *Ecophysiology of Photosynthesis*; Schulze, E.-D., Caldwell, M.M., Eds.; Springer: Berlin/Heidelberg, Germany, 1994; pp. 49–70.
58. Sokal, R.R.; Rohlf, F.J. *Biometry*, 4th ed.; WH Freeman & Co: New York, NY, USA, 2011; p. 960.
59. Atkin, O.K.; Bloomfield, K.J.; Reich, P.B.; Tjoelker, M.G.; Asner, G.P.; Bonal, D.; Bönisch, G.; Bradford, M.G.; Cernusak, L.A.; Cosio, E.G.; et al. Global variability in leaf respiration in relation to climate, plant functional types and leaf traits. *New Phytol.* **2015**, *206*, 614–636. [CrossRef] [PubMed]
60. Warton, D.I.; Duursma, R.A.; Falster, D.S.; Taskinen, S. smart 3- an R package for estimation an inference about allometric lines. *Methods Ecol. Evol.* **2012**, *3*, 257–259. [CrossRef]
61. R Core Team. *R: A Language and Environment for Statistical Computing*; R Foundation for Statistical Computing: Vienna, Austria, 2015; Available online: <http://www.R-project.org/> (accessed on 3 March 2016).
62. Agathokleous, E.; Watanabe, M.; Eguchi, N.; Nakaji, T.; Satoh, F.; Koike, T. Root production of *Fagus crenata* blume saplings grown in two soils and exposed to elevated CO₂ concentration: An 11-year free-air-CO₂ enrichment (FACE) experiment in northern Japan. *Water Air Soil Pollut.* **2016**, *227*, 187. [CrossRef]
63. Tobita, H.; Uemura, A.; Kitao, M.; Kitaoka, S.; Maruyama, Y.; Utsugi, H. Effects of elevated atmospheric carbon dioxide, soil nutrients and water conditions on photosynthetic and growth responses of *Alnus hirsuta*. *Funct. Plant Biol.* **2011**, *38*, 702–710. [CrossRef]
64. Karonen, M.; Ossipov, V.; Ossipova, S.; Kapari, L.; Loponen, J.; Matsumura, H.; Kohno, Y.; Mikami, C.; Sakai, Y.; Izuta, T.; et al. Effects of elevated carbon dioxide and ozone on foliar proanthocyanidins in *Betula platyphylla*, *Betula ermanii*, and *Fagus crenata* seedlings. *J. Chem. Ecol.* **2006**, *32*, 1445–1458. [CrossRef] [PubMed]

65. Landolt, W.; Buhlmann, U.; Bleuler, P.; Bucher, J.B. Ozone exposure-response relationships for biomass and root/shoot ratio of beech (*Fagus sylvatica*), ash (*Fraxinus excelsior*), Norway spruce (*Picea abies*) and Scot pine (*Pinus sylvestris*). *Environ. Pollut.* **2000**, *109*, 473–478. [[CrossRef](#)]
66. Matyssek, R.; Bytnerowicz, A.; Karlsson, P.E.; Paoletti, E.; Sanz, M.; Schaub, M.; Wieser, G. Promoting the O₃ flux concept for European forest trees. *Environ. Pollut.* **2007**, *146*, 587–607. [[CrossRef](#)]
67. Nikolova, P.S.; Andersen, C.P.; Blaschke, H.; Matyssek, R.; Häberle, K.H. Belowground effects of enhanced tropospheric ozone and drought in a beech/spruce forest (*Fagus sylvatica* L./*Picea abies* [L.] Karst). *Environ. Pollut.* **2010**, *158*, 1071–1078. [[CrossRef](#)]
68. Anderson, C.P.; Ritter, W.; Gregg, J.; Matyssek, R.; Grams, T.E.E. Below-ground carbon allocation in mature beech and spruce trees following long-term, experimentally enhanced O₃ exposure in Southern Germany. *Environ. Pollut.* **2010**, *158*, 2604–2609. [[CrossRef](#)]
69. Kinose, Y.; Fukamachi, Y.; Okabe, S.; Hiroshima, H.; Watanabe, M.; Izuta, T. Nutrient supply to soil offsets the ozone-induced growth reduction in *Fagus crenata* seedlings. *Trees* **2017**, *31*, 259–272. [[CrossRef](#)]
70. Watanabe, M.; Okabe, S.; Kinose, Y.; Hiroshima, H.; Izuta, T. Effects of ozone on soil respiration rate of Siebold's beech seedlings grown under different soil nutrient conditions. *J. Agric. Meteorol.* **2019**, *75*, 39–46. [[CrossRef](#)]
71. Kolb, T.E.; Matyssek, R. Limitation and perspectives about scaling ozone impacts in trees. *Environ. Pollut.* **2001**, *115*, 373–393. [[CrossRef](#)]
72. Watanabe, M.; Hoshika, Y.; Koike, T. Photosynthetic responses of Monarch birch seedlings to differing timing of free air ozone fumigation. *J. Plant Res.* **2014**, *127*, 339–345. [[CrossRef](#)] [[PubMed](#)]



© 2019 by the authors. Licensee MDPI, Basel, Switzerland. This article is an open access article distributed under the terms and conditions of the Creative Commons Attribution (CC BY) license (<http://creativecommons.org/licenses/by/4.0/>).